Biogeosciences Discuss., 7, 3257–3295, 2010
www.biogeosciences-discuss.net/7/3257/2010/
doi:10.5194/bgd-7-3257-2010

Biogeosciences Discussions

Carbon fluxes in natural plankton communities under elevated CO_2 levels: a stable isotope labeling study

A. de Kluijver[1], K. Soetaert[1], K. G. Schulz[2], U. Riebesell[2], R. G. J. Bellerby[3], and J. J. Middelburg[1,4]

[1]Netherlands Institute of Ecology (NIOO-KNAW), Centre for Estuarine and Marine Ecology, P. O. Box 140, 4400 AC Yerseke, The Netherlands
[2]Leibniz Institute for Marine Sciences (IFM-GEOMAR), Düsternbrooker Weg 20, 24105 Kiel, Germany
[3]Bjerknes Centre for Climate Research, University of Bergen, Allégaten 55, 5007 Bergen, Norway
[4]Faculty of Geosciences, Utrecht University, P. O. Box 80021, 3508 TA Utrecht, The Netherlands

Received: 13 April 2010 – Accepted: 16 April 2010 – Published: 6 May 2010

Correspondence to: A. de Kluijver (a.dekluijver@nioo.knaw.nl)

Published by Copernicus Publications on behalf of the European Geosciences Union.

Abstract

The potential impact of rising carbon dioxide (CO_2) on carbon fluxes in natural plankton communities was investigated during the 2005 PeECE III mesocosm study in Bergen, Norway. Triplicate mesocosms, in which a phytoplankton bloom was induced by nutrient addition, were incubated with 1×(~350 µatm), 2×(~700 µatm), and 3× present day CO_2(~1050 µatm) levels for 3 weeks. ^{13}C labeled bicarbonate was added to all mesocosms to follow the transfer of carbon from dissolved inorganic carbon (DIC) into phytoplankton and subsequently heterotrophic bacteria, zooplankton, and settling particles. Isotope ratios of polar lipid fatty acids (PLFA) were used to infer the biomass and production of phytoplankton and bacteria. Phytoplankton PLFA were enriched within one day after label addition, while it took another 3 days before bacteria showed substantial enrichment. Group-specific primary production measurements revealed that coccolithophores grew faster than green algae and diatoms. Elevated CO_2 had a significant positive effect on post-bloom biomass of green algae, diatoms, and bacteria. A simple model based on measured isotope ratios of phytoplankton and bacteria revealed that CO_2 had no significant effect on the carbon transfer efficiency from phytoplankton to bacteria. There was no indication of enhanced settling based on isotope mixing models during the phytoplankton bloom. Our results suggest that CO_2 effects are most pronounced in the post-bloom phase, under nutrient limitation.

1 Introduction

The ocean acts as a strong sink for anthropogenic carbon dioxide (CO_2) and has already absorbed around one third of the anthropogenic emitted CO_2 over the past 200 years (Sabine et al., 2004). The dissolution of CO_2 in the oceans causes a change in seawater carbonate chemistry. The dissolved inorganic carbon pool in seawater consists mainly of bicarbonate with small amounts of carbonate and CO_2. Dissolution of CO_2 will lower the seawater pH and carbonate is shifted towards more bicarbonate and CO_2. The average pH of the ocean has already decreased by about 0.1 units

BGD
7, 3257–3295, 2010

compared to pre-industrial levels; this process is called "ocean acidification". Projected pH changes in the surface ocean are a further decrease of about 0.3–0.4 units by the year 2100, when CO_2 emissions continue to rise at present rates (Caldeira and Wickett, 2003). While the magnitude of the changes in seawater chemistry can be predicted with good precision, our knowledge about the biological consequences of ocean acidification is still rather limited. Most marine organisms studied so far have shown some sensitivity to ocean acidification, although the response is highly species dependent. Stimulating effects of increased CO_2 levels, such as increased carbon fixation have been demonstrated for different phytoplankton taxa such as cyanobacteria (e.g. Hutchins et al., 2007), diatoms (e.g. Riebesell et al., 1993), and coccolithophores (e.g. Riebesell et al., 2000a). In natural plankton community incubations, enhanced primary production at increasing CO_2 levels was observed by Hein and Sand-Jensen (1997). The uptake of inorganic carbon based on DIC removal was found to be higher at higher CO_2 levels (Engel et al., 2005; Riebesell et al., 2007). A shift in community composition with increasing CO_2 in favor of diatoms was observed in natural plankton communities (Tortell et al., 2002; Feng et al., 2009). The various responses of phytoplankton groups to changing CO_2 levels can be attributed to various employment and efficiency of carbon concentrating mechanisms (CCMs) (Giordano et al., 2005). However, enhanced carbon fixation not always resulted in higher standing stocks of biomass (Delille et al., 2005; Schulz et al., 2008).

The discrepancy between an enhanced uptake of inorganic carbon at higher CO_2 levels, while plankton biomass is not increasing, may be the result of higher extracellular release of freshly produced material and concomitant export to depth (Arrigo 2007). As suggested by Delille et al. (2005), Bellerby et al. (2008), and Schulz et al. (2008), biomass increase may have been hidden by higher sinking fluxes at elevated CO_2. It is also well known that uptake of carbon continues when nutrient depletion limits cell division but not primary production (Engel et al., 2004a) and at the end of a phytoplankton bloom, when nutrients are exhausted, there is enhanced carbon exudation (Van Den Meersche et al., 2004).

BGD
7, 3257–3295, 2010

Extracellular release of excess carbon is an important food-source for bacteria and the main connection to the microbial food web (Larsson and Hagström 1979). The effect of CO_2 on the coupling between phytoplankton and heterotrophic bacteria is largely unknown. Previous studies indicate that the response of heterotrophic bacteria to changing CO_2 levels is linked to phytoplankton rather than being a direct effect of pH or CO_2 (Grossart et al., 2006). Moreover, experiments with natural communities of heterotrophic bacteria obtained contradictory results, e.g. an increased bacterial activity of attached bacteria at higher CO_2 was observed by Grossart et al. (2006), but not by Allgaier et al. (2008) and Rochelle-Newall et al. (2004). We hypothesize that an enhanced uptake of dissolved inorganic carbon by phytoplankton at higher CO_2 levels could lead to enhanced carbon exudation and a subsequent enhanced coupling to the microbial food web. The enhanced coupling could be either a shorter time-delay between the increase in phytoplankton and bacterial biomass and a larger proportion of primary production channeled to the microbial food web. However, only part of the carbon released by phytoplankton is taken up by bacteria and processed in the microbial food web. Another part of the dissolved organic matter coagulates and forms marine snow (Passow 2002; Engel et al., 2004b). The response of the microbial food web is strongly dependent on nutrient-availability as explained in Thingstad et al. (2008). The balance between these pathways is of extreme importance in determining the oceans' response to increasing CO_2 levels. While an enhanced coupling between phytoplankton and bacteria would provide a positive feedback to ocean acidification because of respiration, enhanced aggregation and sedimentation would provoke a negative feedback to atmospheric CO_2.

It is difficult to quantify the interactions between phytoplankton and heterotrophic bacteria based on standing stock measurements, because they are the net result of many processes. The combined use of stable isotope labeling and biomarkers provides a very powerful tool to study carbon flows in natural communities (Boschker and Middelburg 2002; Van Den Meersche et al., 2004). By analysis of biomarkers specific for phytoplankton and bacteria and the appearance of label in the biomarkers it is possible

BGD
7, 3257–3295, 2010

to resolve and quantify phytoplankton and bacteria interactions. This study was part of the large Pelagic Ecosystem CO_2 Enrichment study (PeECE III), in which natural plankton communities were exposed to different CO_2 levels in large mesocosms (Riebesell et al., 2007; Schulz et al., 2008). ^{13}C-labeled bicarbonate was added as a tracer to the water column and we subsequently traced ^{13}C in phytoplankton and bacteria in the water column and in particulate material in the sediment traps. A simple isotope model was used to quantify transfer rates from phytoplankton to bacteria. With this stable isotope labeling study we aim to address whether high CO_2 levels affect phytoplankton production and growth, and whether it enhances transfer of freshly produced organic matter to the microbial food web or to depth.

2 Material and methods

2.1 Set-up and sampling

The PeECE III mesocosm experiment was carried out at the Marine Biological Station, University of Bergen, Norway, between 16 May and 10 June 2005. Nine mesocosms (M1 to M9) of 9.5 m deep and with a volume of 27 m^3 each were filled with unfiltered, nutrient-poor post-bloom water from the fjord, and manipulated to achieve 3 different CO_2 levels in triplicate mesocosms by aeration of the water column and the overlying atmosphere with CO_2-enriched air. The partial pressures of carbon dioxide (pCO_2) at the start of the experiment were about 350 µatm (1×CO_2, M7-9), 700 µatm (2×CO_2, M4-6), and 1050 µatm (3×CO_2, M1-3). Nitrate (final concentration 15 µmol l^{-1}) and phosphate (final concentration 0.7 µmol l^{-1}) were added to the mesocosms to initiate a phytoplankton bloom. A more detailed description of the experimental set-up can be found in (Schulz et al., 2008). ^{13}C-labeled bicarbonate was added to the upper 5 m of the mesocosms between day 0 and day 1 to a final addition of ca 2.3 µmol kg^{-1}, corresponding to about 0.1% of total DIC. Water samples for polar lipid fatty acids (PLFA) were taken from the upper layer of each mesocosm daily (day 0–18) or

BGD
7, 3257–3295, 2010

every second day (day 20, 22 and 24). The samples were filtered on pre-combusted GF/F filters and stored frozen until further analysis. Sediment traps were placed in each mesocosm at 7.5 m depth and they were collected every 3 days, on day 4, 7, 10, 13, 16, and 19. Zooplankton was collected on day 0, 9, and 26 from some of the mesocosms.

2.2 PLFA and DIC analysis

The lipids were extracted by a modified Bligh and Dyer method (Bligh and Dyer 1959; Boschker et al., 1998). The lipids were fractionated in different polarity classes by column separation on a heat-activated-silicic acid column and subsequent elution with chloroform, acetone and methanol. The methanol fractions, containing most of the polar-lipid fatty acids, were derivatized to fatty acid methyl esters (FAME). The standards 12:0 and 19:0 were used as internal standards. PLFA concentrations were determined by gas chromatograph–flame ionization detection (GC-FID). The δ^{13}C of individual PLFA were measured using gas chromatography-combustion isotope ratio mass spectrometry (GC-C-IRMS (Middelburg et al., 2000; Van Den Meersche et al., 2004). DIC was analyzed by coulometric titration (Bellerby et al., 2008) and its isotope ratio by IRMS.

2.3 Data analysis

Stable isotope data are expressed in the delta notation (δ^{13}C) relative to VPDB standard and the fraction of ^{13}C was derived from the delta notation. Total amount of label (total ^{13}C) is calculated as

$$\text{total}^{13}\text{C} = (^{13}\text{C}_{\text{sample}} - ^{13}\text{C}_{\text{control}}) \cdot \text{concentration } (\mu\text{g C l}^{-1}) \quad (1)$$

where is the isotope fraction at day 0, see Middelburg et al. (2000) and Van Den Meersche et al. (2004) for details. To be able to directly compare labeling of phytoplankton and bacteria biomass between the different mesocosms, the data were corrected for

BGD
7, 3257–3295, 2010

small differences in initial ^{13}C-DIC concentrations. This correction factor was calculated for each mesocosm as total ^{13}C-DIC at day 1 relative to the average total ^{13}C-DIC of all mesocosms at day 1. The correction factor ranged from 0.75 to 1.09.

Out-gassing of ^{13}C-DIC was calculated according to Delille et al. (2005) with chemical enhancement factors. An approximation of $^{13}CO_2$ (aq) was derived from ^{13}C-DIC as described in Zeebe and Wolf-Gladrow (2001) with fractionation factors from Zhang et al. (1995). The pCO_2 concentrations were measured by Bellerby et al. (2008). An approximation of δCO_2-air of −8‰ was used, because no exact measures were available (Fry, 2006).

The sum of PLFA ai15:0 and i15:0 was used to characterize heterotrophic bacteria and in the section on methodological comparison, the PLFA 18:1*ω*7c was included. The sum of PLFA 22:6*ω*3, 20:5*ω*3, 18:4*ω*3, 18:5(n-3,6,9,12,16), 18:5*ω*3, and 18:*3ω3* were used to characterize phytoplankton dynamics (Boschker and Middelburg 2002; Dijkman and Kromkamp 2006; Dijkman et al., 2009). Phytoplankton dynamics were further divided into diatoms (PLFA 16:2*ω*4, 16:4*ω*1 and 20:*5ω3*), coccolithophorids (PLFA 18:*5ω*3 and 18:5(n-3,6,9,12,16)), and green algae (16:4*ω*3 and 18:3*ω*3) (Dijkman and Kromkamp 2006; Dijkman et al., 2009). Phytoplankton composition based on PLFA was also estimated with the Bayesian compositional estimator (Van Den Meersche et al., 2008) with the input ratio from (Dijkman and Kromkamp 2006). The final step involved conversion from PLFA to cell biomass. Bacterial biomass was calculated using a conversion factor of 0.0059 g C (ai+i)15:0 per g C biomass, which is the product of 0.056 g C PLFA per g C biomass (Brinch Iversen and King 1990; Middelburg et al., 2000) and 0.105 g C ai15:0+i15:0 per g C PLFA (calculated from Boschker et al. (1998) and references cited therein). Calculated in the same way, the sum of ai15:0+i15:0+18:1*ω*7c encompassed 25% of PLFA and the final conversion factor was 0.0137 g C (ai+i15:0, 18:1*ω*7c) per g C biomass. We used a carbon content of 20 fg cell^{-1} to convert bacterial biomass to cells (Lee and Fuhrman 1987). The conversion factors for phytoplankton (groups) were derived from data on fatty acid composition in (Dijkman and Kromkamp, 2006). Chlorophyll *a* (chl *a*) concentrations were

BGD
7, 3257–3295, 2010

converted to biomass assuming a C to chl *a* ratio of 45 based on literature values. Although conversion factors are disputable, they don't affect the general patterns nor inferred transfer dynamics from phytoplankton to bacteria. Group-specific growth rates (μ, d^{-1}) during the bloom (from day 5 to day 9) were calculated as

$$\mu = \ln \frac{^{13}\text{C biomass}_{t+\Delta t}}{^{13}\text{C biomass}_{t}} / \Delta t \quad (2)$$

Data from sediment traps were only analyzed for isotope ratios of specific PLFA and not for concentrations because these were biased due to significant over trapping (Schulz et al., 2008). The material in the traps was subdivided in phytoplankton and bacteria using PLFA, similarly as for the suspended particulate matter. The fraction of material derived from the upper layer in the settled material was calculated with the mixing equation (Fry, 2006). The equation used is

$$f_{\text{upper layer}} = (\delta_{\text{sediment}} - \delta_{\text{control}}) / (\delta_{\text{upper layer}} - \delta_{\text{control}}) \quad (3)$$

where δ_{control} is the isotope ratio at day 0 and $\delta_{\text{upper layer}}$ is the isotope ratio of the pelagic PLFA, averaged over the days of settlement. This fraction provides a measure of exchange between upper and deeper layer and can therefore be used as an indication of sinking.

Zooplankton was determined up to species level. The species *Pseudocalanus elongatus* and *Temora longicornis* were analyzed for stable isotope ratios. Since there were only few measurements on zooplankton, the species were grouped together and treated as total zooplankton and only the $1\times CO_2$ and $3\times CO_2$ treatments were considered for analyses.

2.4 Model

A simple source-sink isotope ratio model was used to determine label transfer from phytoplankton to bacteria (Hamilton et al., 2004; Van Oevelen et al., 2006). The following

BGD
7, 3257–3295, 2010

equation was used

$$\frac{d\delta^{13}C_{bac}}{dt} = r_{bac} \cdot f_{phyto} \cdot \delta^{13}C_{phyto} - r_{bac} \cdot \delta^{13}C_{bac} \quad (4)$$

where r_{bac} = bacteria turnover (d^{-1}) and f_{phyto} = fraction of ^{13}C derived from phytoplankton.

The weighted $\Delta\delta^{13}C$ of phytoplankton were used as a forcing function and the weighted $\Delta\delta^{13}C$ of bacteria was used for model calibration. The original data were used to fit the model, instead of ^{13}C-DIC normalized data, but they would give similar results. The assumption for this model is that biomass is constant with time. The model equations were implemented in R, using the packages FME and deSolve (Soetaert and Petzoldt 2009; Soetaert et al., 2009).

The time sequence of the model was 0–24 days and initial conditions were set to 0. Parameter calibration was done with pseudo-randomization followed by Levenberg -Marquardt algorithm (Press et al., 2001). The parameters were further assessed with the Markov-Chain-Monte-Carlo technique (MCMC) (Gelman et al., 1996). During the MCMC, the model was run 5000 times for each mesocosm, resulting in approximately 1500–1750 accepted runs per mesocosm. The mean and standard deviation were calculated for each parameter.

The dependency of heterotrophic bacteria on recently fixed carbon was also calculated using mean isotope ratios over the last 10 days of the experiment ($\Delta\delta^{13}C_{bac}$/ $\Delta\delta^{13}C_{phyto}$). This simple calculated ratio should approach f_{phyto} at steady-state (Van Oevelen et al., 2006).

2.5 Statistics

Results are reported as mean ± standard deviation. In order to test if measured concentrations of phytoplankton and bacteria differed significantly over time among pCO_2 levels, repeated measures ANOVAs and Tukey HSD post-hoc tests were done using the software Statistica® (stat Soft, Inc., U.S., 2009). Prior to analyses, data were

BGD
7, 3257–3295, 2010

checked for normality and homogeneity of variance. Significant differences in phytoplankton growth rates and model parameters were assessed using one-way ANOVA.

3 Results

3.1 Phytoplankton dynamics

PLFA specific for phytoplankton were used to depict phytoplankton dynamics and their carbon concentrations were converted to total carbon biomass. The addition of nutrients induced a phytoplankton bloom as depicted by both PLFA (Fig. 1a) and chlorophyll *a* (Fig. 1b). During the experiment 3 different phases in phytoplankton dynamics could be observed: before the bloom (day 0–5), the bloom (day 5–9), and the post bloom (after day 9). Based on nutrient dynamics, 4 phases were identified by Riebesell et al. (2008) and Tanaka et al. (2008). From start until day 6, there was no nutrient depletion, during day 7–9 silicate was depleted, during day 10–12 silicate and phosphate were depleted and from day 13 onwards, all nutrients were depleted. The development of the bloom as depicted by PLFA reflects the dynamics of phosphate concentrations. When phosphate became depleted, the phytoplankton bloom collapsed (Fig. 1a, h). Phytoplankton biomass (based on PLFA) was low in the first five days of the experiment, with values $<0.2\,\mathrm{mg\,C\,L^{-1}}$. After day 5 the phytoplankton bloom started and phytoplankton biomass rapidly increased up to $0.71 \pm 0.10\,\mathrm{mg\,C\,L^{-1}}$ at day 9, the peak of the bloom assessed using PLFA (Fig. 1a). The bloom collapsed after day 9 to $0.16 \pm 0.043\,\mathrm{mg\,C\,L^{-1}}$ at day 10 and stayed around this concentration until the end of the experiment. Phytoplankton biomass (based on chl *a*) increased from $0.064 \pm 0.0091\,\mathrm{mg\,C\,L^{-1}}$ at day 0 to $0.55 \pm 0.11\,\mathrm{mg\,C\,L^{-1}}$ at day 10, the peak of the bloom. From then on, the bloom continuously decreased until starting values were reached again around day 16 (Fig. 1b) (Schulz et al., 2008).

No CO_2 effects on phytoplankton concentrations and dynamics were observed before and during the bloom (day 0–9). During the post-bloom the phytoplankton biomass

BGD
7, 3257–3295, 2010

based on PLFA was significantly lower in the 1× CO_2 treatment than in the 2× and 3× CO_2 treatments (repeated measures ANOVA, $p < 0.005$) (Table 1). The largest differences in biomass occurred between day 12 and day 17. The development of phytoplankton biomass as determined with PLFA (Fig. 1a), chl *a* (Fig. 1b) and particulate organic carbon (POC) are summarized in Fig. 2a. The range in biomass is similar for all methods, with values from 0–1.2 mg C L^{-1}. The timing of the bloom, however, is different for all methods. The peak of the bloom was at day 9 with PLFA, at day 10 with chl *a*, and at day 11 for POC.

Phytoplankton was further subdivided into the major phytoplankton groups. Conversion of typical PLFA biomarkers for each group into biomass revealed that diatoms were the most abundant taxa, followed by coccolithophores and a minority of green algae (Fig. 1c, d, e). The different taxa showed a similar response during the incubations, peaking at day 9. Diatom biomass rapidly increased after day 5 up to 0.50 ± 0.081 mg C L^{-1} at the peak of the bloom on day 9. The bloom declined to 0.11 ± 0.048 mg C L^{-1} at day 10 and remained low until the end of the incubations (Fig. 1c). A significant CO_2 effect could be detected in the post-bloom phase. The diatom biomass was significantly higher in the 2× CO_2 and 3× CO_2 treatments than in the 1× CO_2 treatment, similar as for total phytoplankton (repeated measures ANOVA, $p < 0.005$) (Table 1). The CO_2 effect was mainly effective from day 12 to day 17. Coccolithophore biomass rapidly increased after day 5 and reached a peak of 0.19 ± 0.066 mg C L^{-1} at day 9. Coccolithophores declined after the bloom peak to concentrations of 0.047 ± 0.028 mg C L^{-1} at day 10 and remained low during the rest of the experiment (Fig. 1d). The development of coccolithophores in the post-bloom phase was independent of CO_2 (Table 1). The biomass of green algae was much lower than that of diatoms and coccolithophores with a maximum of 0.052 ± 0.0071 mg C L^{-1} at day 9 (Fig. 1e). The development of green algae in the post-bloom phase was dependent on CO_2 levels. Green algal biomass remained higher at elevated CO_2 levels, but only between the 1× and 3× CO_2 treatments were differences significant (repeated measures ANOVA, $p < 0.005$) (Table 1).

BGD
7, 3257–3295, 2010

3.2 Bacterial dynamics

Bacterial dynamics showed more fluctuation than phytoplankton (Fig. 1f). Initially, the bacteria biomass declined to a minimum at day 5 of $0.018 \pm 0.0060\,\mathrm{mg\,C\,L^{-1}}$. At the onset of the phytoplankton bloom, bacterial biomass started to increase. The bacterial biomass based on PLFA reached concentrations of $0.16 \pm 0.051\,\mathrm{mg\,C\,L^{-1}}$ at the bloom peak on day 9 followed by a rapid decline to $0.056 \pm 0.017\,\mathrm{mg\,C\,L^{-1}}$ at day 10 (Fig. 1f). After day 10, bacterial concentrations started to increase again to reach a second peak of $0.18 \pm 0.030\,\mathrm{mg\,C\,L^{-1}}$ at day 18. In the post-bloom phase, the bacterial biomass was significantly higher at 3× CO_2 and 2× CO_2 compared to 1× CO_2 (repeated measures ANOVA, $p < 0.005$) (Table 1). The CO_2 effect was most pronounced between day 12 and day 17.

Bacterial cell abundances as determined by PLFA (this study, Fig. 1f), flow cytometry (FCM) (Paulino et al., 2008), and microscopy (Allgaier et al., 2008) are summarized in Fig. 2b. The range of cell numbers was similar for all methods (10^9–10^{10} cells $\mathrm{L^{-1}}$). However, the development of bacteria during the experiment differed for the three methods. The most striking difference occurred around the phytoplankton peak. While flow cytometry and microscopy revealed a minimum in bacterial abundance, PLFA based numbers showed a maximum in bacterial abundance.

3.3 Labeling

^{13}C-labeled DIC addition resulted in an increase of δ^{13}C-DIC with 100.5 ± 11.9‰, from -1.73 ± 1.01‰ at day 0 up to 98.8 ± 12.5‰ at day 1. The large variation was caused by addition of different amounts of ^{13}C bicarbonate to individual mesocosms. During the experiment, the isotope ratio of DIC gradually decreased in all mesocosms to about 74‰ at day 25. Labeled DIC concentrations were $2.29\,\mu\mathrm{mol\,C\,L^{-1}}$ at day 1 and gradually decreased to $1.62 \pm 0.05\,\mu\mathrm{mol\,C\,L^{-1}}$ at day 25 (Fig. 3a). The decrease in labeled DIC was independent of CO_2 levels. The loss of label from gas exchange between water and air was calculated only for the first 5 days, when biomass was still low. Label

BGD
7, 3257–3295, 2010

loss due to gas exchange was negligible for all treatments (<0.1%). A large part of labeled DIC was lost due to mixing with the deeper water layers. Assuming a mixing efficiency of 12% as calculated in Schulz et al. (2008), mixing with the deeper layers could explain 63 ± 10% of label loss.

The transfer from DIC to phytoplankton was very rapid; label enrichment in phytoplankton-specific PLFA was already detectable at day 1. The labeling of phytoplankton steadily increased from day 1 onwards and reached a maximum of 86.9 ± 10.4‰ at day 10, denoting that phytoplankton carbon reached steady-state with dissolved inorganic carbon. The ratios of phytoplankton isotope signature relative to DIC isotope signature, averaged over the last 10 days (day 15–24), are presented in Table 2. The average value was 1.04 ± 0.033 over all mesocosms, implying complete turnover of algal biomass during the experimental period. The development of label incorporation into phytoplankton matched with total phytoplankton dynamics; the labeled biomass was low in the first 5 days and then increased to a bloom peak at day 9 of $0.67 \pm 0.10\,\mu g\,C\,L^{-1}$. The labeled biomass rapidly declined to $0.15 \pm 0.046\,\mu g\,C\,L^{-1}$ at day 10 and remained around this level until the end of the experiment (Fig. 3c). Similar to non-labeled biomass, labeled phytoplankton biomass in the post-bloom phase was significantly higher in the 2× CO_2 and 3× CO_2 treatments than in the 1× CO_2 treatment (repeated measures ANOVA, $p < 0.01$) (Table 1). The effect was most pronounced from day 12 to day 17.

The labeling of the different phytoplankton groups was similar to labeling of total phytoplankton. Labeling of the different phytoplankton groups is presented as an average of all mesocosms in Fig. 3c. The CO_2 effects on the different phytoplankton groups were similar as for non-labeled biomass. Significant CO_2 effects were found in the post-bloom phase for diatoms, where biomass was higher in the 3× and 2× CO_2 treatments than in the 1x CO_2 incubations (repeated measures ANOVA, $p < 0.005$) and for green algae, where biomass was significantly higher in the 3x CO_2 treatment compared to the 1× CO_2 treatment (repeated measures ANOVA, $p = 0.01$) (Table 1). The specific growth rate during the bloom, as determined from label incorporation in biomass from

BGD
7, 3257–3295, 2010

day 5 to day 9, was highest for coccolithophores with a value of $0.76 \pm 0.11\,d^{-1}$, followed by green algae ($0.63 \pm 0.11\,d^{-1}$), and diatoms ($0.59 \pm 0.054\,d^{-1}$) (Fig. 4). Total phytoplankton growth rate was $0.64 \pm 0.075\,d^{-1}$. The growth rate of coccolithophores was significantly higher than the growth rates of green algae and diatoms (ANOVA, $p = 0.001$). Although the growth rates for each single group were not significantly affected by CO_2 treatment, it appeared that for coccolithophores, green algae and total phytoplankton, the growth rate was highest under current CO_2 levels (1× CO_2) (Fig. 4).

The transfer of label to bacteria was much slower than the label transfer from DIC to phytoplankton. It was only at day 3 or 4, depending on the mesocosm, that enrichment could be detected in bacterial specific PLFA (Fig. 3d and 5). Average enrichment was 3.9 ± 3.1‰ on day 3 and 7.4 ± 5.8‰ on day 4. The isotope ratio steadily increased until 72.3 ± 8.8 at day 14, denoting isotope equilibrium. The ratios of bacterial isotope signature to phytoplankton isotope signature over the last 10 days (day 15–day 24) are presented in table 2 for each mesocosm. The average ratio over all mesocosms was 0.87 ± 0.017 implying that 87% of the bacterial carbon was derived from recently fixed phytoplankton material. The other 13% was derived from non-labeled material. The dynamics of labeled bacteria were comparable with non-labeled bacteria; biomass was low in the first 5 days and showed some fluctuation in time. The peak in biomass was reached at day 18 with concentrations of $0.14 \pm 0.022\,\mu g\,C\,L^{-1}$ and declined afterwards (Fig. 3c). Similar to non-labeled bacterial biomass, labeled biomass was significantly higher in the post-bloom phase in 3× CO_2 and 2× CO_2 treatments compared to 1× CO_2 and the effect was mainly present between day 12 and 17 (repeated measures ANOVA, $p < 0.05$) (Table 1).

3.4 Model

The transfer from phytoplankton to bacteria was quantified using a simple source-sink model (Eq. 1). The initial parameters range was $0–1\,d^{-1}$ for both r_{bac} and f_{phyto}. The Bayesian approach produced a good fit to the data of all mesocoms (Fig. 5) and we

BGD
7, 3257–3295, 2010

were able to individually fit the parameters. Because of the large number of MCMC runs, reliable parameter distributions were obtained. The solid black lines are the model output, using the medians of the modeled bacterial ratios. The dark grey areas represent the 95% posterior limits of the model uncertainties. The light grey areas present the 95% posterior limits in predicting new observations (Malve et al., 2005; Malve et al., 2007). The turn-over rates for bacteria (r_{bac}) were $0.20 \pm 0.01\,d^{-1}$, $0.21 \pm 0.02\,d^{-1}$, and $0.23 \pm 0.04\,d^{-1}$, for 1× CO_2, 2× CO_2, 3× CO_2 treatments respectively (Table 2). The fractions of bacterial carbon derived from phytoplankton (f_{phyto}) were $0.92 \pm 0.02\,d^{-1}$, $0.91 \pm 0.02\,d^{-1}$, $0.89 \pm 0.03\,d^{-1}$, for 1× CO_2, 2× CO_2, 3× CO_2 treatments respectively (Table 2). The parameters were not significantly different for the different CO_2 treatments, but a trend with CO_2 concentrations could be observed. The value of f_{phyto} decreased with increasing CO_2 concentrations and the value of r_{bac} increased with increasing CO_2 concentrations.

3.5 Settled material

The isotope ratios of the material in the sediment traps were used to investigate whether sinking of organic matter from the upper layer to the deeper layer in the mesocosms was affected by the different treatments. The average isotope ratios of biomarker PLFA from the upper layer and the average isotope ratio of unlabeled PLFA (day 0) were used in the isotope mixing model to calculate the fraction in the traps derived from the upper layer. The fraction represents the exchange of material between upper and deeper layers. The fraction increased in time and was 0.29 ± 0.051 at day 4 and gradually increased to 0.90 ± 0.028 at day 16 for phytoplankton (Fig. 6a). Exchange was slightly faster in the beginning for bacterial PLFA than for phytoplankton PLFA. The fraction for bacteria was already 0.43 ± 0.12 at day 7, while it was only 0.33 ± 0.030 for phytoplankton. The exchange for bacteria gradually increased to 0.80 ± 0.077 at day 19 (Fig. 6b). Isotope mixing, which is an indication for sinking, was independent of CO_2 treatment.

BGD
7, 3257–3295, 2010

3.6 Zooplankton

Zooplankton was enriched on day 9 with a $\Delta\delta^{13}C$ of 44.2 ± 3.5‰ (3× CO_2) and 41.8 ± 9.3‰ (1× CO_2). At the end of the experiment, at day 26, zooplankton was enriched with 64.6 ± 3.4‰ (3×CO_2) and 59.7 ± 13.8‰ (1× CO_2). The enrichment in zooplankton was not significantly different between the high and low CO_2 treatment.

4 Discussion

The combined use of stable isotopes and biomarkers provides a powerful tool to elucidate and quantify carbon fluxes in natural plankton communities, especially in perturbation experiments (Boschker and Middelburg 2002; Van Den Meersche et al., 2004; Pace et al., 2007). Here we applied the combined technique to determine the uptake of dissolved inorganic carbon by phytoplankton and subsequent transfer within the plankton community under different CO_2 levels. To our best knowledge, this is the first time that this approach is used to directly examine the transfer from phytoplankton to bacteria under changing CO_2 levels. The broad range of measured parameters provided the opportunity to adequately describe the community response and to validate the use of PLFA as biomarkers. The high reproducibility of data between the different mesocosms resulted in robust outcomes of this experiment.

4.1 Phytoplankton and bacterial dynamics

The addition of inorganic nutrients initiated a phytoplankton bloom. The collapse of the bloom coincided with phosphate depletion at day 10 (Fig. 1a, h). The phytoplankton biomass at the bloom peak based on PLFA was ~0.7 mg C L^{-1}, which corresponds to a moderate bloom. The peak in phytoplankton biomass as observed with PLFA occurred earlier (day 9) than the observed peak with chlorophyll *a* (day 10) and POC (day 11) (Fig. 2a). The disagreement between bloom dynamics revealed with chlorophyll *a* and PLFA is most likely due to function and structure of biomarkers and their turn-over after

BGD
7, 3257–3295, 2010

cell death. PLFA are structural components of the cell membrane that rapidly decay after cell death. Phosphate is required to produce PLFA and hence PLFA production is limited by phosphate. In contrast, pigments are used for photosynthesis and require nitrogen. Phosphate exhaustion (day 10) occurred before nitrogen depletion (day 13), which could explain the observed time difference in maximum concentration of phytoplankton PLFA and pigments (Figs. 1, 2a). Possible explanations for the rapid decay of PLFA (Fig. 2a) compared to chl *a* could be cell death with still intact chloroplasts, cell leaking of PLFA or remodeling of the PLFA into other lipids under nutrient limitation. Not all PLFA were lost due to decay or remodeling, since detritus sinking into the sediment traps contained phytoplankton PLFA, suggesting some preservation of PLFA in organic matter. Based on the available data we cannot fully explain the difference in dynamics. The use of cell viability tests are recommended in future experiments to determine the health state of the cells after the bloom collapse. Consistent with pigment data (Riebesell et al., 2007; Schulz et al., 2008), PLFA data revealed that the bloom was dominated by prymnesiophytes (or coccolithophores) and diatoms (Fig. 1c, d, e). The group-specific dynamics, however, were different between pigment and PLFA analysis. In our study, no difference in diatom and coccolithophores succession was observed with PLFA. However, Riebesell et al. (2007), showed that diatoms peaked 1–2 days before coccolithophores, based on pigment analyses. The difference in succession of diatoms and coccolithophores with HPLC can be explained by earlier depletion of silicate (day 7) compared to phosphate (day 10) (Fig. 1h) (Schulz et al., 2008). Phytoplankton cell numbers for different groups were determined in this study with flow cytometry, but showed much more variability in time than PLFA and pigment analyses. Interestingly, coccolithophores showed a bloom peak at day 7 based on FCM data (Paulino et al., 2008) in contrast to HPLC (day 10) and PLFA (day 9) (Fig. 1d) (Riebesell et al., 2007). POC reflects the total organic carbon pool including extracellular polymeric substances and phytoplankton detritus, which explains the ongoing build-up after the bloom peak (Fig. 2a). Label incorporation into PLFA has proven to be a valuable tool to determine group-specific growth rates (Dijkman et al., 2009). High

BGD
7, 3257–3295, 2010

net growth rates were observed during the bloom with coccolithophores growing significantly faster than green algae and diatoms (Fig. 3). Our findings agree with the results obtained with the dilution method combined with pigment analysis during PeECE III, where prymnesiophytes growth rates were higher than diatom growth rates during the bloom (Suffrian et al., 2008).

The collapse of the phytoplankton bloom did not result in a noticeable increase in bacterial biomass and we did not observe a distinct heterotrophic phase in the second part of the experiment (Fig. 1f). Bacterial dynamics correlated with phytoplankton dynamics during the phytoplankton bloom, with simultaneous higher concentrations of phytoplankton and bacteria. Overall, bacterial biomass increased during the experiment. In the PeECE III experiment, bacteria dynamics were also determined by microscopy (Allgaier et al., 2008) and flow cytometry (FCM) (Paulino et al., 2008). Bacterial dynamics based on PLFA biomarkers revealed a different pattern compared to dynamics based on microscopy and FCM. Bacteria were most abundant at day 18–20, when measured with PLFA. In contrast, bacterial dynamics based on microscopic counting and flow cytometry showed a peak at day 12–16 (Allgaier et al., 2008) (Fig. 2b), pointing towards a heterotrophic response to the bloom collapse. A striking difference between the different methods was visible at day 9, the day of the phytoplankton peak bloom. While microscopy and flow cytometry showed a minimum in bacterial numbers, PLFA showed a peak in bacterial abundance. This discrepancy is probably caused by underestimation of bacterial number by FCM and microscopy due to shading by phytoplankton and a large number of phytoplankton-attached bacteria.

The use of PLFA as biomarkers in ocean acidification studies has to be further validated, since their concentration can be pH dependent. The PLFA concentration in bacterial cells for example was found to correlate with pH in soil samples, although the pH range used in that study was much larger than the one used here and in general in ocean acidification studies (Frostegård and Bååth 1996). Culture incubation studies with green algae under different CO_2 (and pH) levels revealed no difference in PLFA concentrations and composition between CO_2 levels (de Kluijver et al., unpublished

BGD
7, 3257–3295, 2010

data), while *Emiliania huxleyi* fatty acid composition was sensitive to changes in pCO_2 (Riebesell et al., 2000b). From a paleo-climatological view it is interesting to find pH dependent biomarkers (more resistant than PLFA), since they can be used as proxies to construct ancient CO_2 sea levels.

4.2 Phytoplankton – bacteria coupling

With improved knowledge of the role of heterotrophic bacteria in the surface ocean, it was recognized that they are major contributors to the recycling of organic matter in the surface ocean, and the concept of the microbial loop was born (Azam et al., 1983). The microbial loop starts with the bacterial consumption of dissolved organic matter (DOM) produced by all components of the food web, and terminates with the consumption of bacteria by small zooplankton. Globally about half of the primary production is routed through DOM and processed by bacteria (Azam et al., 1983). The close relationship between phytoplankton and bacteria has been demonstrated through the existence of robust, general relationships between the abundance and production of bacteria and phytoplankton (Duarte et al., 2005). A substantial part (around 20%) of freshly produced organic matter is shunted to pelagic bacteria through exudation of organic carbon (e.g. Cole et al., 1988).

Based on ^{13}C label dynamics, we observed a transfer from fresh produced phytoplankton material to heterotrophic bacteria. The label was detected in bacteria 2–3 days after incorporation in phytoplankton. At the end of the experiment 87% of bacterial carbon was derived from newly produced phytoplankton material (Fig. 3, Table 2). Overall the first part of the isotope curves mainly reflect uptake and turn-over dynamics, whereas the latter parts of the labeling experiment reflect food source clarification (Fry, 2006). To quantify and test turn-over dynamics and food source clarification in relation to CO_2 levels we applied a simple source-sink model as used in (Hamilton et al., 2004; Carpenter et al., 2005; Van Oevelen et al., 2006). In this model it is assumed that loss processes do not affect the isotope ratio (Figs. 1f, 3d). This is correct only if losses (e.g. bacterial respiration) operate on the bulk tissue. The sources however dilute the

BGD
7, 3257–3295, 2010

isotopic composition of the bacteria with the signature of the source compartment. We chose to assess the interactions with this simple model, with a few parameters, because it was possible to directly test the effect of CO_2 on the parameters of the system. In the first 7 days the model slightly overestimates the isotope ratio of bacteria (Fig. 5). The explanation for this is that f_{phyto} is in fact not constant in time; it will change in response to phytoplankton abundance.

The parameters obtained with our model are remarkably consistent with values described previously. Bacterial turn-over rates based on phytoplankton production ranged from 0.19 d^{-1} to 0.27 d^{-1} with an average of 0.21 d^{-1} in this study (Table 2). These rates represent the net production of bacterial biomass per organic carbon assimilated, also named bacterial growth efficiency (BGE). Del Giorgio et al. (1997) reported a median bacterial growth efficiency of 0.24 d^{-1}, based on modeling of existing data. Del Giorgio and Cole (1998) also reported an average BGE of 0.22 d^{-1} in the oceans in a review on existing data from the literature. An average bacterial production of 20% of primary production was found in a literature survey by Cole et al. (1988). Bacterial cell populations grew on average with 0.28 d^{-1} in culture experiments of Ducklow et al. (1999). The fraction of bacterial biomass derived from phytoplankton products ranged from 0.86 to 0.94 with an average of 0.91, meaning that 91% of carbon in bacteria was coming from freshly produced phytoplankton material and 9% of other food sources. The model derived dependency factors (f_{phyto}) are slightly higher than those based on the ratio $\Delta\delta^{13}C_{bac}/\Delta\delta^{13}C_{phyto}$ (Table 2), because of a slight decrease in bacterial isotope ratios at the end of the experiment. The dependency factor clearly revealed that bacteria also used the algal carbon just fixed prior to incubation or used the unlabeled, background DOC pool. Another explanation could be the presence of an inactive bacteria population. Measurements of ^{13}C-DOC are required to unravel these possibilities.

Few studies have used tracer dynamics and combined modeling to estimate carbon fluxes in natural plankton communities, making comparison limited. A similar estimation of fluxes has been reported by Lyche et al. (1996) who traced ^{14}C in different size fractions as probes for primary and secondary production in a mesocosm study with

BGD
7, 3257–3295, 2010

lake communities. Their values were slightly different from ours (Table 2), with bacteria assimilation rates of 0.485 d^{-1} and a fraction of 0.704 derived from the phytoplankton. Van Den Meersche et al. (2004) studied phytoplankton-bacteria interactions in a tracer experiment with estuarine water and used similar techniques as in this study. They found a 100% dependency of bacteria on freshly produced phytoplankton material, revealed by similar isotope ratios in bacteria and phytoplankton PLFA at the end of the experiment. A similar experiment was conducted by Norrman et al. (1995), where the isotope ratio in bacteria was measured in bacterial nucleic acids. At the end of their incubations, isotope ratios in bacteria were lower than the isotope ratio of POC.

We observed a delay of 2–3 days in transfer from phytoplankton to bacteria in all mesocosms (Fig. 5). The time lag is consistent with previous studies on phytoplankton-bacteria coupling. Duarte et al. (2005) observed a time-lag of 0–4 days between phytoplankton production and bacterial production in Southern Ocean plankton incubations. Ducklow et al. (1999) also observed lag periods of several days in bacterial response to phytoplankton bloom development in Southern Ocean plankton incubations. Van Den Meersche et al. (2004) observed a ~1 day delay in labeling of bacteria compared to phytoplankton. Studies on biomass standing stocks of phytoplankton and bacteria during phytoplankton spring blooms also revealed some uncoupling and delay in response of bacteria to phytoplankton, varying from several days to weeks (Kirchman et al., 1994; Lochte et al., 1997), while a close coupling was observed by Lancelot and Billen (1984). There are several possible explanations for these "lags" or "uncoupling". The most obvious explanation is the presence of unlabeled DOM at the start of the experiment, which is later replenished by labeled DOM. DOM release by phytoplankton can occur passively (leakage and viral lysis) or actively under nutrient starvation (Van Den Meersche et al., 2004). Possibly, DOM release was low in the first part of the experiment (before and during the bloom) because it occurred mainly passively and the major DOM release took place during the bloom collapse, although this was not reflected in standing-stock measurements of DOC (Schulz et al., 2008). Other explanations that concern more the physiological state of the bacteria have been summarized

BGD
7, 3257–3295, 2010

by Ducklow et al. (1999). They suggested that most, if not all, marine bacteria exist predominantly in a state of dormancy, under severe carbon, phosphate, and/or energy starvation. Another possibility is that the apparent lag phase is a reflection of logistic (s-shaped) growth curves. A third scenario concerns the hypothetical existence of non-dividing subpopulations of cells which are progressively overgrown by the growing populations. The high dependency of bacteria on phytoplankton (Table 2) and the small increase in DOM standing stocks (Schulz et al., 2008) during the experiment indicate a strong coupling between phytoplankton and heterotrophic bacteria. Probably there was strong grazing pressure on bacteria that kept the bacterial standing stock low. Bacterivory was indeed high during the experiment as determined by measuring uptake of fluorescent labeled bacteria by protists (Tanaka et al., unpublished data).

4.3 Sinking of fresh produced material

The establishment of the halocline separated the surface layer and deep layer and the sediment traps were located in the deep layer. Unfortunately, windy conditions caused mixing of the water in the mesocosms and resuspension of already settled material, especially on day 12 when a heavy storm occurred (Schulz et al., 2008). These circumstances made it difficult to use absolute numbers of phytoplankton and bacterial biomass in the sediment traps. Consequently we limit our analysis to isotope ratios and to the first 12 days, which can still give us some insight in sinking of freshly produced material. Mixing between the upper and deeper layer was not so important, since at day 10 only about half of the material in the sediment traps was derived from the upper layer (Fig. 6). An interesting observation is that bacteria derived material settled more rapid than phytoplankton material. Close relationships exist between bacteria and detritus. Bacteria rapidly colonize detritus and enhance further aggregation of detritus and subsequent sinking (e.g. Biddanda and Pomeroy 1988). Because of turnover of PLFA after phytoplankton death, the detritus will contain less phytoplankton PLFA and there is thus a preferential sinking of bacteria over phytoplankton (as determined with PLFA), which could be another explanation for the low standing stock in

BGD
7, 3257–3295, 2010

bacteria (Figs. 1f and 2b). Because POC consists both of living biomass and detritus, the stable isotope ratio of POC would be a better source for estimating organic matter dynamics. During this study we did not measure ^{13}C content of POC, so we could only use phytoplankton PLFA.

5 CO_2 effects and implications for ocean acidification

In this study, we aimed to advance our understanding into the effect of elevated pCO_2 levels on phytoplankton and bacterial dynamics and on the interaction between them. Furthermore we aimed to gain insight to the effect of CO_2 on sinking of freshly produced material. Our results clearly showed an effect of CO_2 on total and labeled standing stocks of bacteria and phytoplankton in the post-bloom phase, but not on carbon transfer from DIC to phytoplankton and subsequently bacteria and zooplankton. Unfortunately, during the post-bloom phase a heavy storm mixed the mesocosms, making it difficult to quantify settling processes. The phytoplankton bloom was independent of CO_2 concentrations in this study (Figs. 1 and 3). These results agree with other results obtained in PeECE III on phytoplankton bloom development. Phytoplankton bloom development based on pigments (Riebesell et al., 2007; Schulz et al., 2008), flow cytometry (Paulino et al., 2008), and particulate organic carbon (Schulz et al., 2008) was also found to be CO_2 independent during the PeECE III mesocosm experiment. Previous CO_2 enrichment mesocosm studies also showed little effect on particulate organic matter production, although the effect of CO_2 is species dependent. In PeECEI, some phytoplankton groups like coccolithophores were sensitive to changes in CO_2, where other groups like diatoms were not (Delille et al., 2005; Engel et al., 2005). We also found reduced growth rates of coccolithophores under elevated compared to present day pCO_2 levels (Fig. 4), but this difference was not significant (p = 0.22). In agreement with our findings, in the PeECE I experiment the coccolithophore *Emiliania huxleyi* also showed reduced growth rates with increasing CO_2 levels (Engel et al., 2005). The growth rate of diatoms was unaffected by CO_2 in this study. The results agree with

BGD
7, 3257–3295, 2010

previous results from coastal plankton assemblages on diatom growth rates (Tortell et al., 2000), although it can be species dependent as shown by Kim et al. (2006).

Interestingly, we did observe CO_2 related effects in the post-bloom phase of the experiment. Green algae and diatoms seemed to benefit from increased pCO_2 as their biomass was significantly higher under high CO_2 levels in the post-bloom phase (Fig. 1, Table 1). Current CO_2 levels are generally considered to be a non-limiting resource for diatoms and green algae, because they have efficient carbon concentrating mechanisms (CCMs) (Giordano et al., 2005). But the production of these mechanisms requires energy, so when energy becomes limited, higher CO_2 concentrations can be beneficial. In a recent study from Feng et al. (2009), diatom abundance increased with increasing pCO_2 in shipboard community incubations. Moreover, Egge et al. (2009) reported higher total community primary production rates in the post-bloom phase of the PeECE III experiments in high CO_2 treatments.

We found no indication of enhanced sinking of phytoplankton at increasing CO_2 levels based on isotope ratios in the sediment traps (Fig. 6). However, the results should be interpreted with caution. Sinking of freshly produced material would mainly occur during and after the bloom collapse and we don't have reliable sediment trap data for that period due to the storm event. An enhanced carbon consumption was based on DIC budgets (Riebesell et al., 2007; Bellerby et al., 2008), but was not reflected in standing stocks of biological material. The concentrations of TEP (Egge et al., 2009), POC and DOC were independent of CO_2 (Schulz et al., 2008). Riebesell et al. (2007) suggested that the discrepancy may have been caused by an enhanced particle sinking. Unfortunately, our sediment trap data could not be used to confirm or falsify this hypothesis.

The development of bacterial biomass showed a similar response to CO_2 as phytoplankton, with a significantly higher biomass at higher CO_2 in the post-bloom phase compared to present pCO_2 levels (Figs. 1f and 3d, Table 1). In the post-bloom phase, our results concerning bacterial dynamics differ from those of other bacteria results from PeECE III studies. No differences in bacterial abundance under the different CO_2

BGD
7, 3257–3295, 2010

levels were observed with flow cytometry and with microscopy (Allgaier et al., 2008; Paulino et al., 2008). Previous studies have shown that the response of heterotrophic bacteria to changing CO_2 levels is linked to phytoplankton rather than being a direct effect of pH or CO_2 (e.g. Grossart et al., 2006). The increased biomass at higher pCO_2 could be a direct result of increased phytoplankton biomass at higher pCO_2. We did not observe enhanced coupling between phytoplankton and bacteria under higher pCO_2 with the isotope model (Fig. 5, Table 2). The coupling could only be studied before and during the bloom, because of label saturation in the post-bloom phase. Since CO_2 effects manifested in the post-bloom phase, the effect was not visible in the model parameters. Remarkably, the dependency of bacteria on phytoplankton tended to decrease with increasing CO_2 (Table 2), consistent with a scenario that more carbon is routed into export at high CO_2 levels (Riebesell et al., 2007). Tracer addition experiments in nutrient-limited plankton incubations or tracer addition in the post-bloom phase can contribute to our understanding of the effect of CO_2 on phytoplankton-bacteria coupling.

Acknowledgements. The authors gratefully acknowledge the staff of the Espegrend Marine Biological Station, University Bergen, in particular T. Sørlie and A. Aadnesen, and the Bergen Marine Research infrastructure (RI) for helping organize and set up the mesocosm experiment. PeEceIII team members are thanked for the stimulating environment and for providing access to data. We thank Ulysses S. Ninnemann for technical support on DIC analyses. Marco Houtekamer and Pieter van Rijswijk are greatly acknowledged for their work on PLFA extractions and analyses. We thank Dick van Oevelen, Frederik de Laender, Eric Boschker, and Jacco Kromkamp for their help with data analyses. Thanks to Francesc Montserrat and Peter Herman for helping with statistical analyses. This study received financial support from the European Project on Ocean Acidification (EPOCA, FP7, 2211384) and the Darwin Center for Biogeosciences supported by the Netherlands Organisation for Scientific Research.

BGD
7, 3257–3295, 2010

References

Allgaier, M., Riebesell, U., Vogt, M., Thyrhaug, R., and Grossart, H.-P.: Coupling of heterotrophic bacteria to phytoplankton bloom development at different pCO_2 levels: a mesocosm study, Biogeosciences, 5, 1007–1022, 2008, http://www.biogeosciences.net/5/1007/2008/.

Arrigo, K. R.: Carbon cycle – Marine manipulations, Nature, 450, 491–492, 2007.

Azam, F., Fenchel, T., Field, J. G., Gray, J. S., Meyerreil, L. A., and Thingstad, F.: The ecological role of water-column microbes in the sea, Mar. Ecol.-Prog. Ser., 10, 257–263, 1983.

Bellerby, R. G. J., Schulz, K. G., Riebesell, U., Neill, C., Nondal, G., Heegaard, E., Johannessen, T., and Brown, K. R.: Marine ecosystem community carbon and nutrient uptake stoichiometry under varying ocean acidification during the PeECE III experiment, Biogeosciences, 5, 1517–1527, 2008, http://www.biogeosciences.net/5/1517/2008/.

Biddanda, B. A. and Pomeroy, L. R.: Microbial aggregation and degradation of phytoplankton-derived detritus in seawater. 1. Microbial succession, Mar. Ecol.-Prog. Ser., 42, 79–88, 1988.

Bligh, E. G. and Dyer, W. J.: A rapid method of total lipid extraction and purification, Can. J. Biochem. Phys., 37, 911–917, 1959.

Boschker, H. T. S. and Middelburg, J. J.: Stable isotopes and biomarkers in microbial ecology, Fems Microbiol. Ecol., 40, 85–95, 2002.

Boschker, H. T. S., Nold, S. C., Wellsbury, P., Bos, D., de Graaf, W., Pel, R., Parkes, R. J., and Cappenberg, T. E.: Direct linking of microbial populations to specific biogeochemical processes by ^{13}C-labelling of biomarkers, Nature, 392, 801–805, 1998.

Brinch Iversen, J. and King, G. M.: Effects of substrate concentration, growth-state, and oxygen availability on relationships among bacterial carbon, nitrogen and phospholipid phosphorus-content, Fems Microbiol. Ecol., 74, 345–355, 1990.

Caldeira, K. and Wickett, M. E.: Anthropogenic carbon and ocean pH, Nature, 425, 365–365, 2003.

Carpenter, S. R., Cole, J. J., Pace, M. L., Van de Bogert, M., Bade, D. L., Bastviken, D., Gille, C. M., Hodgson, J. R., Kitchell, J. F., and Kritzberg, E. S.: Ecosystem subsidies: Terrestrial support of aquatic food webs from ^{13}C addition to contrasting lakes, Ecology, 86, 2737–2750, 2005.

Cole, J. J., Findlay, S., and Pace, M. L.: Bacterial production in fresh and saltwater ecosytstems

BGD
7, 3257–3295, 2010

- A cross-system overview, Mar. Ecol.-Prog. Ser., 43, 1–10, 1988.
del Giorgio, P. A., Cole, J. J., and Cimbleris, A.: Respiration rates in bacteria exceed phytoplankton production in unproductive aquatic systems, Nature, 385, 148–151, 1997.
del Giorgio, P. A. and Cole, J. J.: Bacterial growth efficiency in natural aquatic systems, Annu. Rev. Ecol. Syst., 29, 503–541, 1998.
Delille, B., Harlay, J., Zondervan, I., Jacquet, S., Chou, L., Wollast, R., Bellerby, R. G. J., Frankignoulle, M., Borges, A. V., Riebesell, U., and Gattuso, J. P.: Response of primary production and calcification to changes of pCO_2 during experimental blooms of the coccolithophorid Emiliania huxleyi, Global Biogeochem. Cy., 19(14), Gb2023, doi:10.1029/2004gb002318, 2005.
Dijkman, N. A. and Kromkamp, J. C.: Phospholipid-derived fatty acids as chemotaxonomic markers for phytoplankton: application for inferring phytoplankton composition, Mar. Ecol.-Prog. Ser., 324, 113–125, 2006.
Dijkman, N., Boschker, H., Middelburg, J., and Kromkamp, J. C.: Group-specific primary production based on stable-isotope labeling of phospholipid-derived fatty acids, Limnol. Oceanogr.-Meth., 7, 612–625, 2009.
Duarte, C. M., Agusti, S., Vaque, D., Agawin, N. S. R., Felipe, J., Casamayor, E. O., and Gasol, J. M.: Experimental test of bacteria-phytoplankton coupling in the Southern Ocean, Limnol. Oceanogr., 50, 1844–1854, 2005.
Ducklow, H., Carlson, C., and Smith, W.: Bacterial growth in experimental plankton assemblages and seawater cultures from the Phaeocystis antarctica bloom in the Ross Sea, Antarctica, Aquat. Microb. Ecol., 19, 215–227, 1999.
Egge, J. K., Thingstad, T. F., Larsen, A., Engel, A., Wohlers, J., Bellerby, R. G. J., and Riebesell, U.: Primary production during nutrient-induced blooms at elevated CO_2 concentrations, Biogeosciences, 6, 877–885, 2009, http://www.biogeosciences.net/6/877/2009/.
Engel, A., Zondervan, I., Aerts, K., Beaufort, L., Benthien, A., Chou, L., Delille, B., Gattuso, J. P., Harlay, J., Heemann, C., Hoffmann, L., Jacquet, S., Nejstgaard, J., Pizay, M. D., Rochelle-Newall, E., Schneider, U., Terbrueggen, A., and Riebesell, U.: Testing the direct effect of CO_2 concentration on a bloom of the coccolithophorid Emiliania huxleyi in mesocosm experiments, Limnol. Oceanogr., 50, 493–507, 2005.
Engel, A., Delille, B., Jacquet, S., Riebesell, U., Rochelle-Newall, E., Terbruggen, A., and Zondervan, I.: Transparent exopolymer particles and dissolved organic carbon production by

BGD
7, 3257–3295, 2010

Emiliania huxleyi exposed to different CO_2 concentrations: a mesocosm experiment, Aquat. Microb. Ecol., 34, 93–104, 2004a.
Engel, A., Thoms, S., Riebesell, U., Rochelle-Newall, E., and Zondervan, I.: Polysaccharide aggregation as a potential sink of marine dissolved organic carbon, Nature, 428, 929–932, 2004b.
Feng, Y. Y., Hare, C. E., Leblanc, K., Rose, J. M., Zhang, Y. H., DiTullio, G. R., Lee, P. A., Wilhelm, S. W., Rowe, J. M., Sun, J., Nemcek, N., Gueguen, C., Passow, U., Benner, I., Brown, C., and Hutchins, D. A.: Effects of increased pCO_2 and temperature on the North Atlantic spring bloom. I. The phytoplankton community and biogeochemical response, Mar. Ecol.-Prog. Ser., 388, 13–25, doi:10.3354/meps08133, 2009.
Frostegård, A. and Bååth, E.: The use of phospholipid fatty acid analysis to estimate bacterial and fungal biomass in soil, Biol. Fert. Soils, 22, 59–65, 1996.
Fry, B.: Stable isotope ecology, ed. Springer Science and Business Media, 2006.
Gelman, A.: Inference and monitoring convergence, in: Markov Chain Monte Carlo in Practice, edited by: Gilks, W. R., Richardson, S., and Spiegelhalter, D. J., London, UK, Chapman& Hall, p. 131–140, 1996.
Giordano, M., Beardall, J., and Raven, J. A.: CO_2 concentrating mechanisms in algae: Mechanisms, environmental modulation, and evolution, Annu. Rev. Plant Biol., 56, 99–131, 2005.
Grossart, H. P., Allgaier, M., Passow, U., and Riebesell, U.: Testing the effect of CO_2 concentration on the dynamics of marine heterotrophic bacterioplankton, Limnol. Oceanogr., 51, 1–11, 2006.
Hamilton, S. K., Tank, J. L., Raikow, D. F., Siler, E. R., Dorn, N. J., and Leonard, N. E.: The role of instream vs allochthonous N in stream food webs: modeling the results of an isotope addition experiment, J. N. Am. Benthol. Soc., 23, 429–448, 2004.
Hein, M. and Sand-Jensen, K.: CO_2 increases oceanic primary production, Nature, 388, 526–527, 1997.
Hutchins, D. A., Fu, F. X., Zhang, Y., Warner, M. E., Feng, Y., Portune, K., Bernhardt, P. W., and Mulholland, M. R.: CO_2 control of Trichodesmium N_2 fixation, photosynthesis, growth rates, and elemental ratios: Implications for past, present, and future ocean biogeochemistry, Limnol. Oceanogr., 52, 1293–1304, 2007.
Kim, J. M., Lee, K., Shin, K., Kang, J. H., Lee, H. W., Kim, M., Jang, P. G., and Jang, M. C.: The effect of seawater CO_2 concentration on growth of a natural phytoplankton assemblage in a controlled mesocosm experiment, Limnol. Oceanogr., 51, 1629–1636, 2006.

BGD
7, 3257–3295, 2010

Kirchman, D. L., Ducklow, H. W., McCarthy, J. J., and Garside, C.: Biomass and nitrogen uptake by heterotrophic bacteria during the spring phytoplankton bloom in the North-Atlantic ocean, Deep-Sea Res. Pt. I, 41, 879–895, 1994.
Lancelot, C. and Billen, G.: Activity of heterotrophic bacteria and its coupling to primary production during the spring phytoplankton bloom in the southern bight of the North-sea, Limnol. Oceanogr., 29, 721–730, 1984.
Larsson, U. and Hagstrom, A.: Phytoplankton Exudate Release as an Energy-Source for the Growth of Pelagic Bacteria, Mar. Biol., 52, 199–206, 1979.
Lee, S. and Fuhrman, J. A.: Relationships between biovolume and biomass of naturally derived marine bacterioplankton, Appl. Environ. Microbiol., 53, 1298–1303, 1987.
Lochte, K., Bjornsen, P. K., Giesenhagen, H., and Weber, A.: Bacterial standing stock and production and their relation to phytoplankton in the Southern Ocean, Deep-Sea Res. Pt. II, 44, 321–340, 1997.
Lyche, A., Andersen, T., Christoffersen, K., Hessen, D. O., Hansen, P. H. B., and Klysner, A.: Mesocosm tracer studies. 2. The fate of primary production and the role of consumers in the pelagic carbon cycle of a mesotrophic lake, Limnol. Oceanogr., 41, 475–487, 1996.
Malve, O., Laine, M., and Haario, H.: Estimation of winter respiration rates and prediction of oxygen regime in a lake using Bayesian inference, Ecol. Model., 182, 183–197, doi:10.1016/j.ecolmodel.2004.07.020, 2005.
Malve, O., Laine, M., Haario, H., Kirkkala, T., and Sarvala, J.: Bayesian modelling of algal mass occurrences - using adaptive MCMC methods with a lake water quality model, Environmental Modelling & Software, 22, 966–977, doi:10.1016/j.envsoft.2006.06.016, 2007.
Middelburg, J. J., Barranguet, C., Boschker, H. T. S., Herman, P. M. J., Moens, T., and Heip, C. H. R.: The fate of intertidal microphytobenthos carbon: An in situ C-13-labeling study, Limnol. Oceanogr., 45, 1224–1234, 2000.
Norrman, B., Zweifel, U. L., Hopkinson, C. S., and Fry, B.: Production and utilization of dissolved organic carbon during an experimental diatom bloom, Limnol. Oceanogr., 40, 898–907, 1995.
Pace, M. L., Carpenter, S. R., Cole, J. J., Coloso, J. J., Kitchell, J. F., Hodgson, J. R., Middelburg, J. J., Preston, N. D., Solomon, C. T., and Weidel, B. C.: Does terrestrial organic carbon subsidize the planktonic food web in a clear-water lake?, Limnol. Oceanogr., 52, 2177–2189, 2007.
Passow, U.: Transparent exopolymer particles (TEP) in aquatic environments, Prog. Oceanogr.,

BGD
7, 3257–3295, 2010

55, 287–333, 2002.
Paulino, A. I., Egge, J. K., and Larsen, A.: Effects of increased atmospheric CO_2 on small and intermediate sized osmotrophs during a nutrient induced phytoplankton bloom, Biogeosciences, 5, 739–748, 2008, http://www.biogeosciences.net/5/739/2008/.
Press, W., Teukolsky, S., Vetterling, W., and Flannery, B.: Numerical recipes: the art of scientific computing, Cambridge Univ Pr, 2007.
Riebesell, U., Wolfgladrow, D. A., and Smetacek, V.: Carbon-dioxide limitation of marine-phytoplankton growth-rates, Nature, 361, 249–251, 1993.
Riebesell, U., Zondervan, I., Rost, B., Tortell, P. D., Zeebe, R. E., and Morel, F. M. M.: Reduced calcification of marine plankton in response to increased atmospheric CO_2, Nature, 407, 364-367, 2000a.
Riebesell, U., Schulz, K. G., Bellerby, R. G. J., Botros, M., Fritsche, P., Meyerhöfer, M., Neill, C., Nondal, G., Oschlies, A., Wohlers, J., and Zöllner, E.: Enhanced biological carbon consumption in a high CO_2 ocean, Nature, 450, 545–549, 2007.
Riebesell, U., Bellerby, R. G. J., Grossart, H.-P., and Thingstad, F.: Mesocosm CO_2 perturbation studies: from organism to community level, Biogeosciences, 5, 1157–1164, 2008, http://www.biogeosciences.net/5/1157/2008/.
Riebesell, U., Revill, A. T., Holdsworth, D. G., and Volkman, J. K.: The effects of varying CO_2 concentration on lipid composition and carbon isotope fractionation in Emiliania huxleyi, Geochim. Cosmochim. Acta, 64, 4179–4192, 2000b.
Rochelle-Newall, E., Delille, B., Frankignoulle, M., Gattuso, J. P., Jacquet, S., Riebesell, U., Terbruggen, A., and Zondervan, I.: Chromophoric dissolved organic matter in experimental mesocosms maintained under different pCO_2 levels, Mar. Ecol.-Prog. Ser., 272, 25–31, 2004.
Sabine, C. L., Feely, R. A., Gruber, N., Key, R. M., Lee, K., Bullister, J. L., Wanninkhof, R., Wong, C. S., Wallace, D. W. R., Tilbrook, B., Millero, F. J., Peng, T. H., Kozyr, A., Ono, T., and Rios, A. F.: The oceanic sink for anthropogenic CO_2, Science, 305, 367–371, 2004.
Schulz, K. G., Riebesell, U., Bellerby, R. G. J., Biswas, H., Meyerhöfer, M., Müller, M. N., Egge, J. K., Nejstgaard, J. C., Neill, C., Wohlers, J., and Zöllner, E.: Build-up and decline of organic matter during PeECE III, Biogeosciences, 5, 707–718, 2008, http://www.biogeosciences.net/5/707/2008/.
Soetaert, K. and Petzoldt, T.: FME: A Flexible Modelling Environment for inverse modelling,

BGD
7, 3257–3295, 2010

sensitivity, identifiability, monte carlo analysis, R package version, 1, 2009.
Soetaert, K., Petzoldt, T., and Setzer, R. W.: deSolve: General solvers for initial value problems of ordinary differential equations (ODE), partial differential equations (PDE) and differential algebraic equations (DAE), R package version, 1, 2009.
Suffrian, K., Simonelli, P., Nejstgaard, J. C., Putzeys, S., Carotenuto, Y., and Antia, A. N.: Microzooplankton grazing and phytoplankton growth in marine mesocosms with increased CO_2 levels, Biogeosciences, 5, 1145-1156, 2008, http://www.biogeosciences.net/5/1145/2008/.
Tanaka, T., Thingstad, T. F., Lvdal, T., Grossart, H.-P., Larsen, A., Allgaier, M., Meyerhöfer, M., Schulz, K. G., Wohlers, J., Zöllner, E., and Riebesell, U.: Availability of phosphate for phytoplankton and bacteria and of glucose for bacteria at different pCO_2 levels in a mesocosm study, Biogeosciences, 5, 669–678, 2008, http://www.biogeosciences.net/5/669/2008/.
Thingstad, T., Bellerby, R., Bratbak, G., Børsheim, K., Egge, J., Heldal, M., Larsen, A., Neill, C., Nejstgaard, J., and Norland, S.: Counterintuitive carbon-to-nutrient coupling in an Arctic pelagic ecosystem, Nature, 455, 387–390, 2008.
Tortell, P. D., DiTullio, G. R., Sigman, D. M., and Morel, F. M. M.: CO_2 effects on taxonomic composition and nutrient utilization in an Equatorial Pacific phytoplankton assemblage, Mar. Ecol.-Prog. Ser., 236, 37–43, 2002.
Tortell, P. D., Rau, G. H., and Morel, F. M. M.: Inorganic carbon acquisition in coastal Pacific phytoplankton communities, Limnol. Oceanogr., 45, 1485–1500, 2000.
Van den Meersche, K., Middelburg, J. J., Soetaert, K., van Rijswijk, P., Boschker, H. T. S., and Heip, C. H. R.: Carbon-nitrogen coupling and algal-bacterial interactions during an experimental bloom: Modeling a ^{13}C tracer experiment, Limnol. Oceanogr., 49, 862–878, 2004.
Van den Meersche, K., Soetaert, K., and Middelburg, J. J.: A Bayesian compositional estimator for microbial taxonomy based on biomarkers, Limnol. Oceanogr.-Meth., 6, 190–199, 2008.
van Oevelen, D., Moodley, L., Soetaert, K., and Middelburg, J. J.: The trophic significance of bacterial carbon in a marine intertidal sediment: Results of an in situ stable isotope labeling study, Limnol. Oceanogr., 51, 2349–2359, 2006.
Zeebe, R. E. and Wolf-Gladrow, D. A.: CO_2 in Seawater: Equilibrium, Kinetics, Isotopes, Elsevier Science, 2001.
Zhang, J., Quay, P. D., and Wilbur, D. O.: Carbon-isotope fractionation during gas-water exchange and dissolution of CO_2, Geochim. Cosmochim. Acta, 59, 107–114, 1995.

BGD
7, 3257–3295, 2010

Table 1. Average non-labeled biomass (mg C l^{-1}) and labeled biomass (µg C l^{-1}) of major phytoplankton groups and bacteria the post-bloom phase (day 10–day 24) with p-values from post-hoc analyses after repeated measures ANOVA.

Organism	Value	1×CO_2	2×CO_2	3×CO_2	p1×, 2×	p1×, 3×
Total phytoplankton	Biomass	0.13	0.15	0.17	0.0071	0.0012
	Labeled biomass	0.12	0.14	0.15	0.047	0.0080
Diatoms	Biomass	0.066	0.085	0.090	0.014	0.0047
	Labeled biomass	0.054	0.067	0.07	0.014	0.0035
Coccolithophores	Biomass	0.030	0.032	0.034	NS*	NS*
	Labeled biomass	0.027	0.028	0.029	NS*	NS*
Green algae	Biomass	0.011	0.014	0.017	NS*	0.0026
	Labeled biomass	0.0089	0.012	0.015	NS*	0.0085
Bacteria	Biomass	0.086	0.11	0.12	0.012	0.0021
	Labeled biomass	0.067	0.083	0.089	0.047	0.010

* NS, not significant

BGD
7, 3257–3295, 2010

Table 2. Model parameters and steady-state ratios for each mesocosm ± standard deviation.

Mesocosm	r_{bac} (model)	f_{phyto} (model)	$\Delta\delta_{phytoplankton}/\Delta\delta^{1}_{DIC}$	$\Delta\delta_{bacteria}/\Delta\delta^{1}_{phytoplankton}$
7–1×CO_2	0.197 ± 0.0305	0.924 ± 0.0427	1.05	0.882
8–1×CO_2	0.197 ± 0.0291	0.908 ± 0.0434	1.03	0.857
9–1×CO_2	0.208 ± 0.0230	0.942 ± 0.0370	1.00	0.905
Average 1×CO_2	0.201 ± 0.00667	0.925 ± 0.0170	1.03 ± 0.023	0 ± 0.0241
4–2×CO_2	0.208 ± 0.0267	0.921 ± 0.0356	1.01	0.885
5–2×CO_2	0.191 ± 0.0243	0.925 ± 0.0375	1.02	0.879
6–2×CO_2	0.230 ± 0.0516	0.888 ± 0.0513	1.10	0.851
Average 2×CO_2	0.209 ± 0.0195	0.911 ± 0.0203	1.04 ± 0.050	0.872 ± 0.0181
1–3×CO_2	0.270 ± 0.0475	0.860 ± 0.0371	1.04	0.857
2–3×CO_2	0.223 ± 0.0258	0.904 ± 0.0258	1.02	0.873
3–3×CO_2	0.192 ± 0.0303	0.920 ± 0.0410	1.08	0.864
Average 3×CO_2	0.228 ± 0.0395	0.895 ± 0.0308	1.04 ± 0.031	0.865 ±0.00769

[1] average ratios over the last 10 days (day 15–24)

BGD
7, 3257–3295, 2010

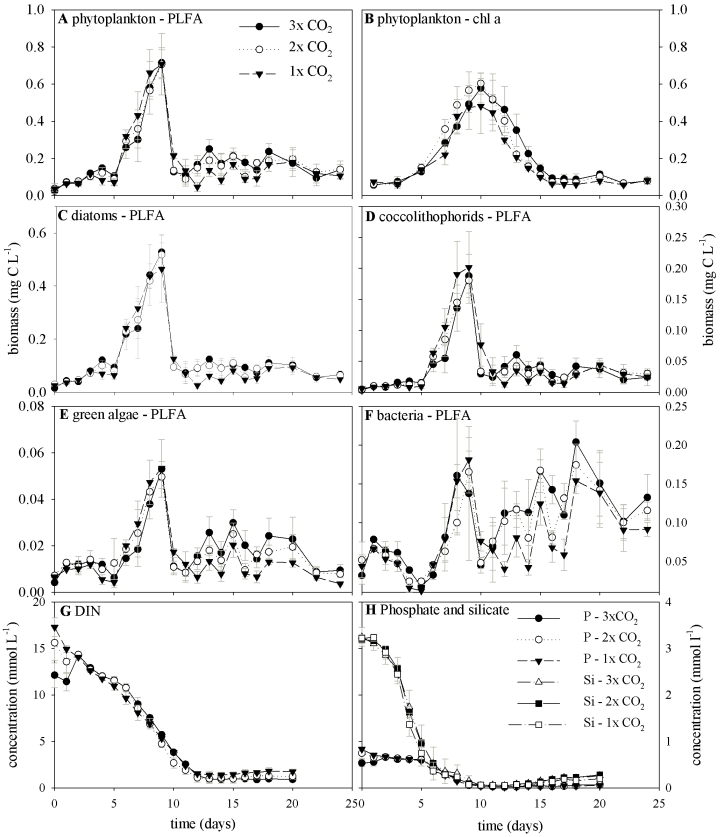

Fig. 1. Concentrations of **(A)** total phytoplankton carbon based on PLFA, **(B)** total phytoplankton carbon based on chlorophyll *a* and PLFA derived carbon estimates for **(C)** diatoms, **(D)** coccolithophores, **(E)** green algae, **(F)** bacteria. Concentrations of **(G)** dissolved inorganic nitrogen, **(H)** phosphate and silicate in the different CO_2 treatments. Average and SD of the three replicates are shown.

BGD
7, 3257–3295, 2010

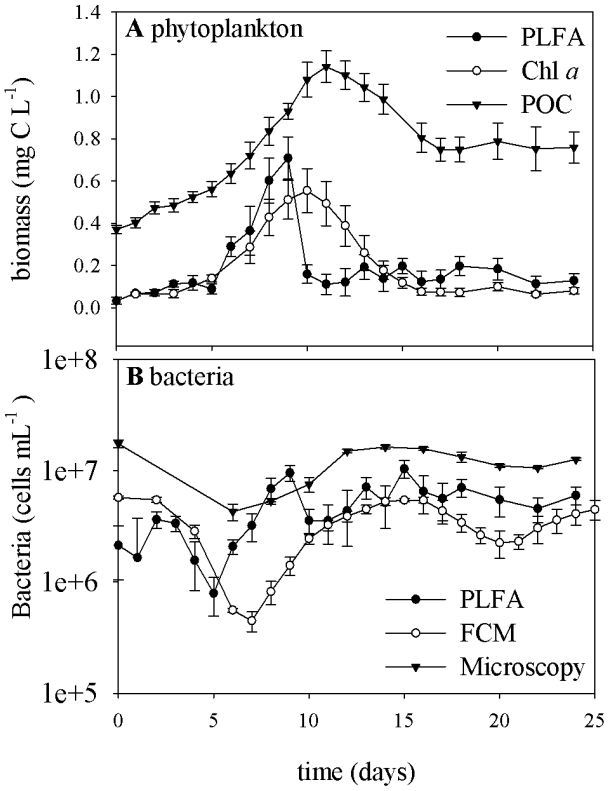

Fig. 2. Comparison of **(A)** phytoplankton biomass based on PLFA, Chl *a*, and POC and **(B)** bacterial numbers based on PLFA, Flow Cytometry (FCM), and microscopy. Average and SD of all mesocosms are shown.

BGD
7, 3257–3295, 2010

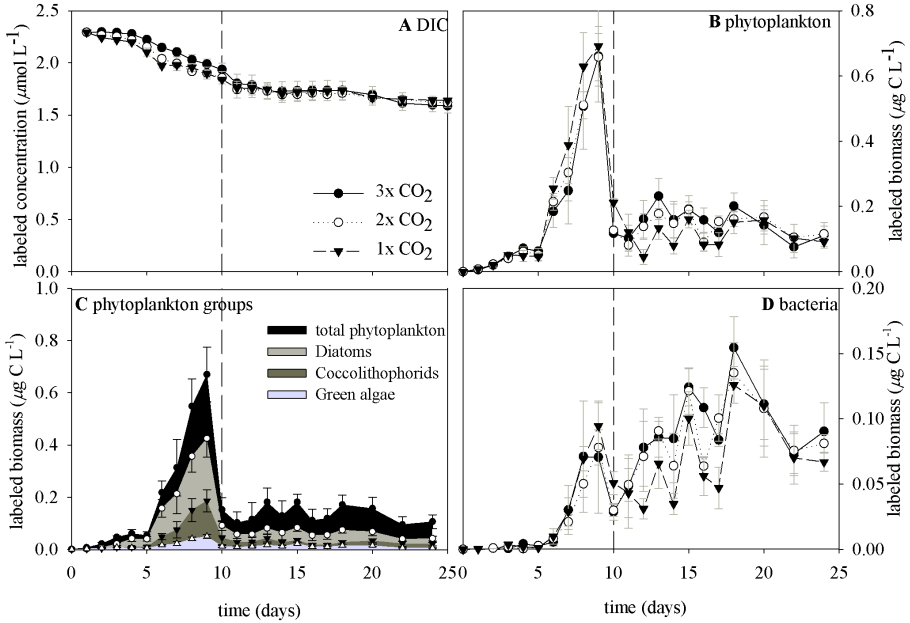

Fig. 3. Concentrations of ^{13}C labeled **(A)** DIC, **(B)** phytoplankton, phytoplankton groups **(C)**, and **(D)** bacteria. Average and SD of the three replicates are shown for (A–C) and average and SD of all mesocosm data are shown in (D).

BGD
7, 3257–3295, 2010

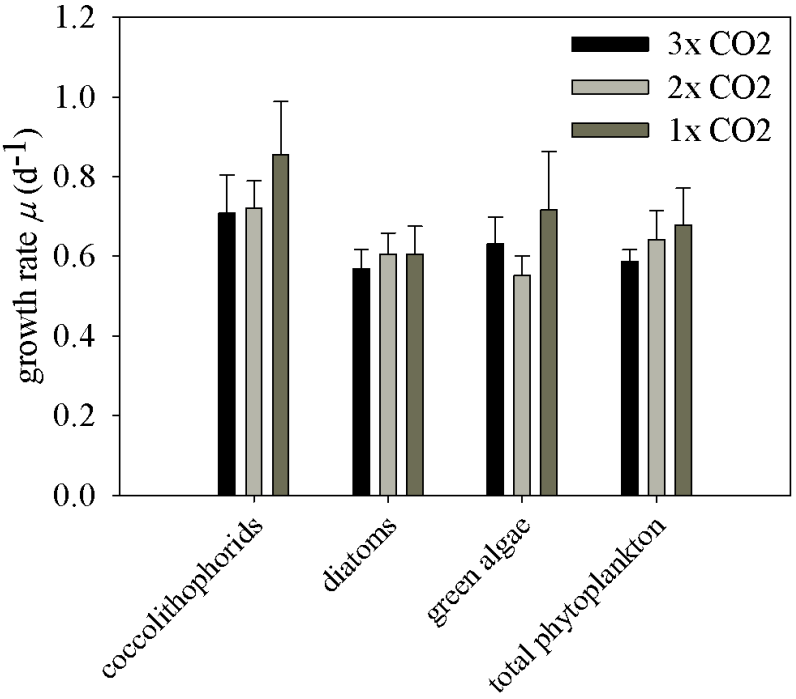

Fig. 4. Phytoplankton group-specific growth rates during the bloom period, day 5–9. Average and SD are shown.

BGD
7, 3257–3295, 2010

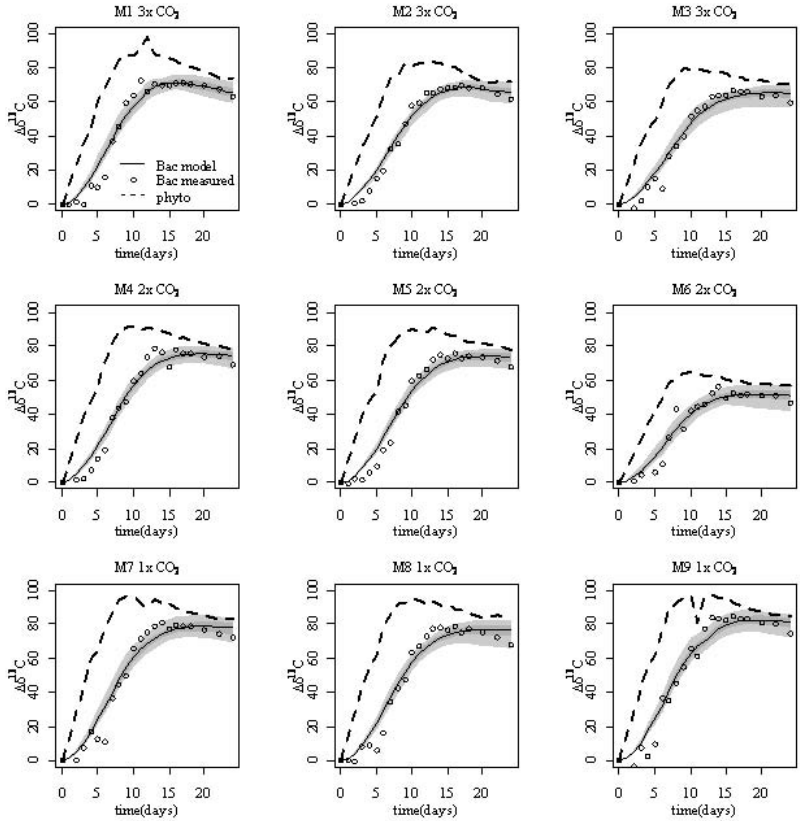

Fig. 5. Model simulations of ^{13}C transfer from phytoplankton to heterotrophic bacteria for individual mesocosms. Phytoplankton $\Delta\delta^{13}C$ data (dashed line) are used as forcing function for model prediction (solid line; Bacteria (Bac) model) of bacterial $\Delta\delta^{13}C$ data (open dots; Bac measured). Dark and light grey areas give 95% limits on model uncertainty and in predicting new observations, respectively (see text).

BGD
7, 3257–3295, 2010

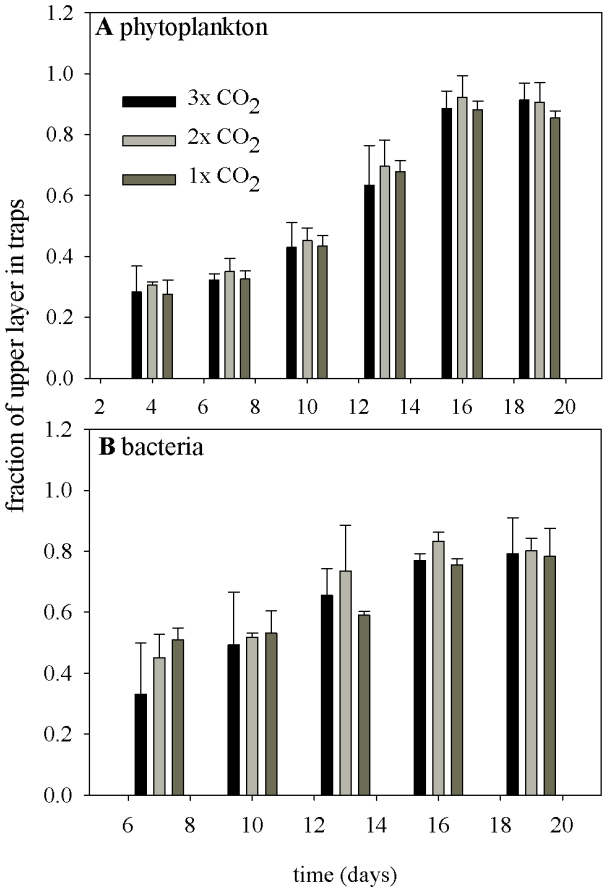

Fig. 6. The fractions in the sediment traps derived from the upper layer for **(A)** phytoplankton and **(B)** bacteria. Average and SD are shown for the triplicate mesocosms.

BGD
7, 3257–3295, 2010